Earth and Planetary Science Letters 273 (2008) 38–47

Contents lists available at ScienceDirect

Earth and Planetary Science Letters

journal homepage: www.elsevier.com/locate/epsl

Novel high-pressure structures of $MgCO_3$, $CaCO_3$ and CO_2 and their role in Earth's lower mantle

Artem R. Oganov [a,b,*], Shigeaki Ono [c], Yanming Ma [a,d], Colin W. Glass [a], Alberto Garcia [e]

[a] Laboratory of Crystallography, Department of Materials ETH Zurich, HCI G 515, Wolfgang-Pauli-Str. 10, CH-8093 Zurich, Switzerland
[b] Geology Department, Moscow State University, 119992 Moscow, Russia
[c] Institute for Research on Earth Evolution, Japan Agency for Marine-Earth Science and Technology, 2-15 Natsushima-cho, Yokosuka-shi, Kanagawa 237-0061, Japan
[d] National Laboratory of Superhard Materials, Jilin University, Changchun 130012, People's Republic of China
[e] Institut de Ciencia de Materials de Barcelona, CSIC, Campus de la UAB, E-08193 Bellaterra, Spain

ARTICLE INFO

Article history:
Received 22 January 2008
Received in revised form 29 May 2008
Accepted 3 June 2008
Available online 14 June 2008

Editor: L. Stixrude

Keywords:
post-magnesite
density functional theory
ab initio simulations
crystal structure prediction
evolutionary algorithm
high pressure

ABSTRACT

Most of the oxidized carbon in the Earth's lower mantle is believed to be stored in the high-pressure forms of $MgCO_3$ and/or $CaCO_3$ or possibly even CO_2. Recently, through *ab initio* evolutionary simulations and high-pressure experiments, a complete picture of phase transformations of $CaCO_3$ at mantle pressures was obtained. Here, using the same approach, we investigate the high-pressure structures of $MgCO_3$. Two new structure types were predicted to be stable in the relevant pressure range: one at 82–138 GPa and the other above 138 GPa. Both phases contain rings of corner-sharing CO_4-tetrahedra. These predictions were largely confirmed by the experiments presented here. A number of structurally very different, but energetically competitive metastable polymorphs were found and reveal complex high-pressure chemistry of $MgCO_3$, in contrast to $CaCO_3$. For CO_2, from 19 GPa to at least 150 GPa, we find β-cristobalite structure to be stable. Differences between high-pressure tetrahedral carbonates and low-pressure silicates are discussed in terms of rigidity of the T–O–T angles (flexible when T=Si and stiff when T=C). We show that through most of the *P–T* conditions of the mantle, $MgCO_3$ is the major host of oxidized carbon in the Earth. We discuss the possibility of CO_2 release at the very bottom of the mantle, which could enhance partial melting of rocks and explain the geodynamical differences between the Earth and Venus.

1. Introduction

High-pressure behaviour of carbonates is very important for the global geochemical carbon cycle. Throughout most of the lower mantle conditions are strongly reducing: indeed, it has been experimentally shown (Frost et al., 2004) and theoretically confirmed (Zhang and Oganov, 2006) that free metallic iron must exist in small amounts in normal pyrolitic mantle. The traditional view (Luth, 1999) is that carbon exists in a reduced form (e.g., diamond) in the normal lower mantle and in the oxidised form (e.g., carbonates) in subducted slabs, where conditions are less reducing. Recent finding of carbonates coming presumably from the lower mantle (Brenker et al., 2007) confirms this picture.

In the reduced regions, depending on the amount of free Fe available, two reactions are possible: $MgCO_3+2Fe=MgO+2FeO+C$ and $MgCO_3+5Fe=MgO+2FeO+Fe_3C$. Using thermodynamic extrapolations, it was suggested (Scott et al., 2001) that the latter reaction is favourable at all mantle conditions. Our calculations, taking into account the new high-pressure structures of $MgCO_3$ found here, suggest both reactions are favourable above 47 GPa (see Supplementary Online Material). At extremely reducing conditions and pressures above 50 GPa cementite (Fe_3C) should be formed instead of diamond; cementite and iron inclusions have been found in ultradeep diamonds from Jagersfontaine, South Africa (A. Jones, personal communication). Oxidised carbon should be the dominant form in subducted slabs and possibly in the uppermost 400–500 km of the lower mantle (pressures below 47 GPa).

Recent experimental work (Shcheka et al., 2006) has convincingly demonstrated that the solubility of carbon in silicates is very small and most of the Earth's oxidised carbon must be hosted by high-pressure forms of Mg and/or Ca carbonates. Decomposition of these carbonates would produce free CO_2 in the mantle, possibly in the fluid phase, and the presence of such volatiles can enhance processes of chemical equilibration, strongly rheologically weaken mantle rocks and cause their partial melting.

A major issue is the high-pressure crystal structures and phase diagrams in the system $MgCO_3$-$CaCO_3$. At ambient conditions there are three stable phases: magnesite ($MgCO_3$), calcite ($CaCO_3$) and dolomite ($CaMg(CO_3)_2$). The latter decomposes into $MgCO_3$ and $CaCO_3$ at pressures of the uppermost mantle (Martinez et al., 1996; Sato and Katsura, 2001; Shirasaka et al., 2002), hence one only needs to study the high-pressure behaviour of $MgCO_3$ and $CaCO_3$. For $CaCO_3$, the

* Corresponding author. Laboratory of Crystallography, Department of Materials ETH Zurich, HCI G 515, Wolfgang-Pauli-Str. 10, CH-8093 Zurich, Switzerland. Tel.: +41 1 632 3752, fax: +41 1 632 1133.
E-mail address: a.oganov@mat.ethz.ch (A.R. Oganov).

0012-821X/$ – see front matter © 2008 Elsevier B.V. All rights reserved.
doi:10.1016/j.epsl.2008.06.005

high-pressure sequence of structures has been predicted (Oganov et al., 2006) and subsequently confirmed (Ono et al., 2007); we briefly discuss this in Section 3.1.

The main questions addressed here are:

1. What are the structures of stable post-magnesite phases of $MgCO_3$? (Section 3.2).
2. How do the new structures extend our understanding of the crystal chemistry of high-pressure carbonates? (Section 3.4).
3. What is the main host of oxidised carbon in the lower mantle? (Section 3.5). To solve this complex problem, one needs to study possible decomposition reactions:

$$MgCO_3 = MgO + CO_2 \quad (R1a)$$

$$CaCO_3 = CaO + CO_2 \quad (R1b)$$

and exchange reactions in excess of SiO_2 (relevant for the basaltic part of subducted slabs):

$$MgCO_3 + SiO_2 = MgSiO_3 + CO_2 \quad (R2a)$$

$$CaCO_3 + SiO_2 = CaSiO_3 = CO_2 \quad (R2b)$$

These reactions determine whether or not free CO_2 can be present in the lower mantle, with far-reaching geochemical and geodynamical implications.

Furthermore, to determine whether it is $MgCO_3$ or $CaCO_3$ that is preferable at conditions of the lower mantle, we consider two more reactions:

$$CaCO_3 + MgSiO_3 = CaSiO_3 + MgCO_3 \quad (R3)$$

$$CaCO_3 + MgO = MgCO_3 + CaO \quad (R4)$$

We note that the latter reactions occur in excess of $MgSiO_3$ and MgO, as expected in the pyrolitic mantle.

4. What is the stable structure of CO_2 at lower mantle pressures (24–136 GPa)? (Section 3.3). Apart from its fundamental interest, this controversial (Yoo et al., 1999; Holm et al., 2000; Dong et al., 2000; Bonev et al., 2003) issue is essential for the study of the reactions (R1a,b–R2a,b). We also explore the stability of CO_2 to decomposition into elemental carbon and oxygen.

To solve problems (1)–(4), we predicted the stable structures of $MgCO_3$ and CO_2 (structures of the other compounds involved in the reactions (R1a,b–R4) are already known) using the newly developed *ab initio* evolutionary methodology (Oganov et al., 2006; Oganov and Glass, 2006; Glass et al., 2006), and support these predictions by high-pressure diffraction experiments on $MgCO_3$. Section 2 describes our methodology, in Section 3 we discuss the results, and a summary is presented in Section 4.

2. Methodology

2.1. Ab initio calculations

Prediction of the stable crystal structure on the basis of only the chemical composition is a very difficult problem (Maddox, 1988) that has remained intractable (Day et al., 2005), except for very simple cases. The recent development of the USPEX (Universal Structure Predictor: Evolutionary Xtallography) method (Oganov et al., 2006; Oganov and Glass, 2006; Glass et al., 2006) was a major step forward, enabling relatively complex systems to be treated. This method is based on a specifically developed evolutionary algorithm featuring real-space representation of structures, local optimisation, and physically motivated flexible variation operators. Tested on several dozen compounds with well-known structures, the method showed a remarkable, nearly 100%, success rate (Oganov and Glass, 2006; Glass et al., 2006). Moreover, it has been successful in predicting a number of new high-pressure structures — e.g., two new phases of $CaCO_3$ (Oganov et al., 2006), a new stable chain structure of sulphur (Oganov and Glass, 2006), structure of metallic ζ-phase of oxygen (Ma et al., 2007), an exotic autoionised phase of boron (Oganov et al., submitted for publication) and new phases of FeS (Ono et al., in press).

Our structure prediction runs for $MgCO_3$ were performed at 110 GPa and 150 GPa, all at zero Kelvin and for systems containing 5, 10, 20, 30 atoms/cell. The population size, depending on the system size, was in the range of 18–70. Evolutionary simulations of CO_2 were done at 50, 100 and 150 GPa, and at each pressure systems with 3, 6, 9, 12, 18 and 24 atoms/cell were studied. The first generation was created randomly (we also explored non-random starting conditions using structures known for other ABX_3 systems or found in smaller simulations of $MgCO_3$). Each newly generated structure was relaxed at constant pressure. The best (i.e. lowest-enthalpy) 50–60% of the structures in each generation participated in producing the next generation through heredity (75–85% of the offspring), atomic permutation (10–15%) and lattice mutation (0–15%). On average, 2–3 atomic swaps were performed during permutation, and the strength of lattice mutation (Oganov and Glass, 2006) was set to 0.5–0.7. In each generation, the best few structures (typically, one) survived and competed in the next generation. Typical structure prediction runs required ~15–50 generations. For $MgCO_3$, largest system sizes (20–30 atoms/cell) proved to be unexpectedly difficult for structure search, which prompted us to repeat simulations several times.

Local optimisations and enthalpy calculations were done fully *ab initio*, using density functional theory within the generalised gradient approximation (GGA) (Perdew et al., 1996) and employing the PAW method (Blöchl, 1994; Kresse and Joubert, 1999) as implemented in the VASP code (Kresse and Furthmüller, 1996). The PAW potentials have $1s^2 2s^2 2p^6$ (core radius 2 a.u.), $1s^2$ (radius 1.5 a.u.) and $1s^2$ (radius 1.52 a.u.) cores for Mg, C and O, respectively. A plane-wave kinetic energy cut-off of 500 eV was used, and demonstrated to give excellent convergence of stress tensors and structural energy differences. To ensure optimal comparability of the calculated enthalpies, for each structure we generated a **k**-points grid with a reciprocal-space resolution of 0.125 $Å^{-1}$ (in some runs 0.10 $Å^{-1}$). Once a set of low-enthalpy structures was found, these structures were relaxed at different pressures in the range of 0–200 GPa using finer **k**-points grids, a more accurate PAW potential for Mg ($1s^2 2s^2$ core, radius 2 a.u.) and plane-wave cut-off of 600 eV; for Ca-bearing compounds we used a PAW potential with the $1s^2 2s^2 2p^6$ core (core radius 2 a.u.).

We also attempted structure prediction using *ab initio* metadynamics (Martoňák et al., 2003; Martoňák et al., 2005, 2006) with SIESTA (Soler et al., 2002) and VASP (Kresse and Furthmüller, 1996) codes, using lattice vectors matrix as (6-dimensional) order parameter. These runs were performed at 150 GPa with 20-, 40- and 80-atom cells starting with the magnesite structure and some of the low-enthalpy structures found here. While there are many cases where metadynamics finds the stable structure (see, e.g., Martoňák et al., 2005; Oganov et al., 2005a), for $MgCO_3$ metadynamics did not produce any energetically competitive structures. This happens when the free energy landscape is highly complex and anisotropic, or lattice vectors are not good order parameters. The structures found were often disordered and typically contained 3-, 4- or often both 3- and 4-coordinate carbon atoms, and had high enthalpies. These runs used the original (Martoňák et al., 2003) formulation of metadynamics; we note that its new "rescaled" formulation (Martoňák et al., 2006) could be more successful. Below we discuss only the structures predicted using the USPEX methodology (Oganov et al., 2006; Oganov and Glass, 2006; Glass et al., 2006).

2.2. High-pressure experiments

We used the laser-heating system of the synchrotron beamlines at Photon Factory and Spring-8 in Japan. A motor-driven diamond anvil

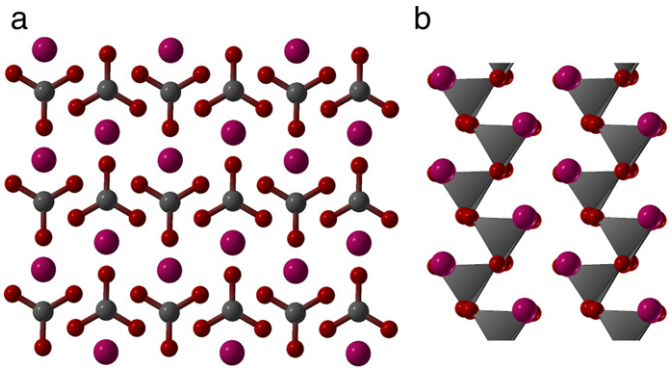

Fig. 1. Structures of high-pressure phases of $CaCO_3$: a) post-aragonite (stable at 42–137 GPa), b) $C222_1$ phase (stable at 137–240 GPa). From Oganov et al. (2006).

cell equipped with 150 μm culet diamonds was used, with a mixture of $MgCO_3$ and gold powder as the starting material. No pressure transmitting medium was used to minimise contamination of the diffraction peaks of the sample. The compacted disk of sample powder of approximate thickness ~20 μm was placed in the 50 μm diameter hole of the rhenium gasket, preindented to a thickness of 20 μm. To reduce metastability problems, the sample was heated by the infrared laser at each pressure increment. The temperatures reached were 1500–2000 K, as measured by the CCD spectrometer in the wavelength range 600–800 nm. The X-ray beam was focused on <30 μm diameter and was also aligned at the centre of the heated spot. The high X-ray flux allowed recording one diffraction spectrum on an imaging plate in 10–20 min. The sample pressure was estimated using the equation of state of gold (Dorogokupets and Oganov, 2007). X-ray wavelengths used in the measurements were 0.41103 and 0.41046 Å at 125 and 143 GPa, respectively.

3. Results and discussion

3.1. High-pressure structures of CaCO3

As a result of several recent studies, pressure-induced transitions of $CaCO_3$ are now well understood. After the well-known transition from calcite to aragonite at ~2 GPa (e.g., Suito et al., 2001; Oganov et al., 2006), there is a transition to a post-aragonite phase at ~40 GPa, the structure of which (Fig. 1a) remained controversial for some time (Ono et al., 2005b; Santillán and Williams, 2004), but was finally solved (Oganov et al., 2006) using USPEX (Oganov et al., 2006; Oganov and Glass, 2006; Glass et al., 2006), and the predicted structure matched well the experimental X-ray diffraction pattern.

Furthermore, we have predicted (Oganov et al., 2006) that above 137 GPa a new phase, with the space group $C222_1$ and containing chains of carbonate tetrahedra (Fig. 1b), becomes stable. Recently this prediction was verified by experiments (Ono et al., 2007) at pressures above 130 GPa. We note that both the post-aragonite and the $C222_1$ structure belong to new structure types and could not be found by analogy with any known structures. The upper limit of stability of this phase was found to be 240 GPa, above which an overcompressed form of aragonite, also with chains of corner-sharing carbonate tetrahedra and with space group *Pmcn*, is more energetically favourable (Arapan et al., 2007). Structures of the novel chain carbonates are different from the known structures of chain silicates and belong to new structure types.

3.2. High-pressure crystal chemistry of CO_2

The high-pressure behaviour of CO_2 is still under debate (Yoo et al., 1999; Holm et al., 2000; Dong et al., 2000; Bonev et al., 2003). It is known that above ~20 GPa a non-molecular phase (called phase V) with tetrahedrally coordinated carbon atoms becomes stable, but its structure is controversial: in the first experimental study (Yoo et al., 1999) a trydimite structure was proposed, but later theoretical works found it to be unstable (not even metastable) and much less favourable than the β-cristobalite structure (Holm et al., 2000; Dong et al., 2000). At the same time, it was not possible to rule out the existence of other, more stable, structures.

Our evolutionary structure searches performed at 50 GPa, 100 GPa and 150 GPa confirmed stability of the β-cristobalite structure (Fig. 2) with space group $I\bar{4}2d$. As to the trydimite structure proposed in (Yoo et al., 1999), we find it to have a much higher enthalpy; *ab initio* molecular dynamics simulations showed that this structure spontaneously decays into a lower-enthalpy disordered state (which is still much less favourable that the β-cristobalite structure). We also find that CO_2-V is stable against decomposition into diamond and oxygen (the enthalpy of decomposition is very large and increases from 3.3 eV to 3.8 eV between 50 GPa and 200 GPa).

At lower pressures, the evolutionary search performed at 15 GPa produces the previously proposed molecular $P4_2/mnm$ structure (see (Bonev et al., 2003) for details). The calculated enthalpy differences (Fig. 2) demonstrate that the $P4_2/mnm$ phase is stable between 8.9 GPa and 18.9 GPa, while at lower pressures (0–8.9 GPa) the molecular *Pa*3 structure is more stable (Fig. 2). The *Pa*3–$P4_2/mnm$ transition pressure calculated here (8.9 GPa) is consistent with experiment and previous calculation (Bonev et al., 2003), which gives further validation to our calculations.

Evolutionary simulations at 50–150 GPa also uncovered several interesting metastable non-molecular (polymeric) forms shown in

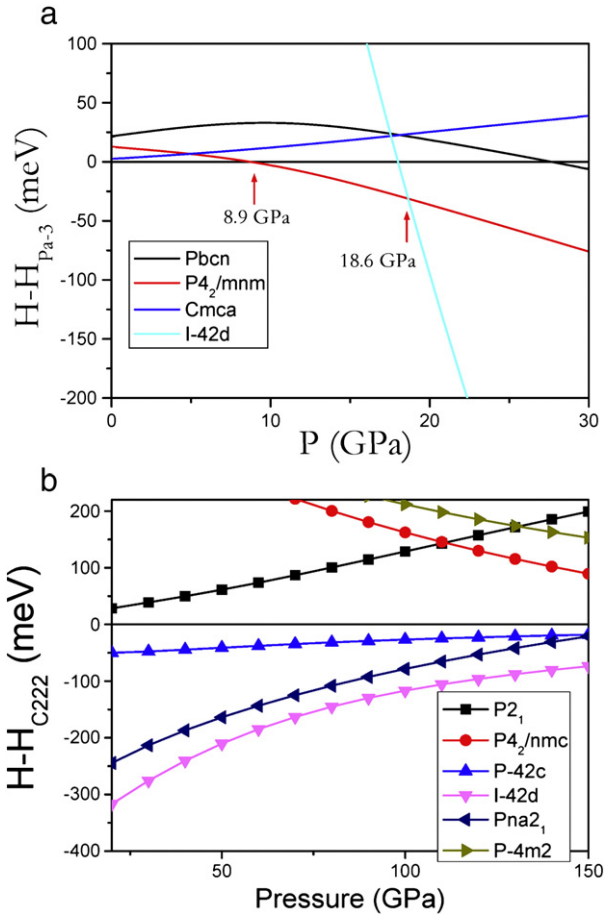

Fig. 2. Enthalpies of candidate polymorphs of CO_2: a) in the low-pressure region (enthalpies are shown per formula unit and relative to the molecular *Pa*3 structure), b) in the high-pressure region (enthalpies are shown per formula unit and relative to the non-molecular *C*222 structure).

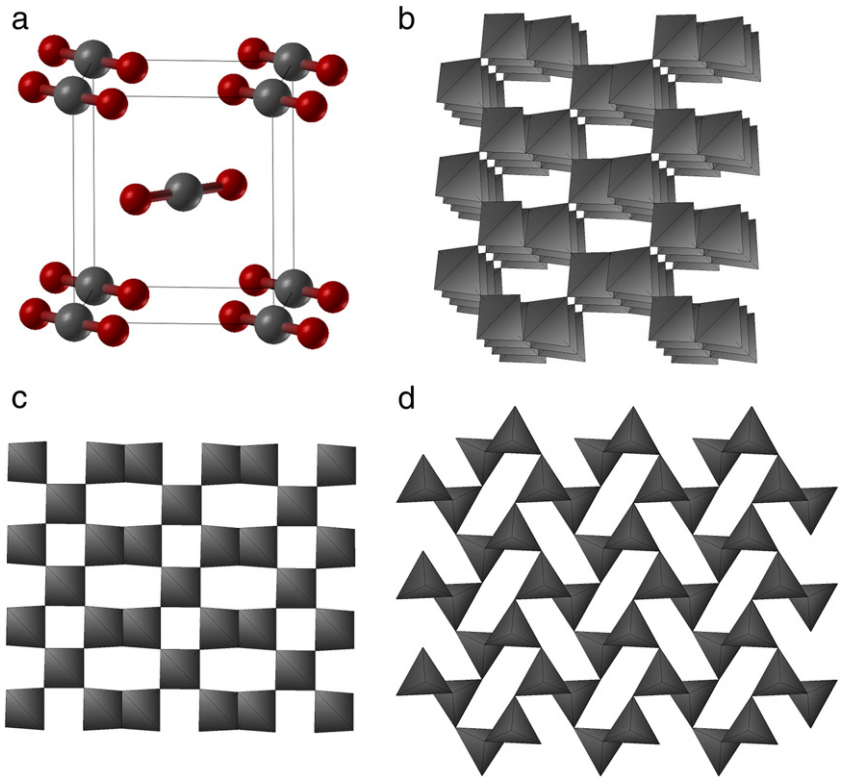

Fig. 3. CO_2 structures: a) molecular $P4_2/mnm$ structure, stable at lower pressures than CO_2-V (8.9–18.6 GPa), b) β-cristobalite-type form of CO_2 at 100 GPa, suggested to be the structure of stable phase V and showing carbonate tetrahedra. Structural parameters at 100 GPa: space group $I\bar{4}2d$, $a=b=3.2906$ Å, $c=6.0349$ Å, C(0.5; 0; 0.25), O(0.2739; 0.25; 0.125), c) metastable polymeric $C222$ structure, d) metastable polymeric $Pna2_1$ structure.

Fig. 3; none of these are known for SiO_2. One can notice that for CO_2, the β-cristobalite structure is much lower in enthalpy compared to other structures — this is again at odds with silica, where a large number of structures with similar energies are known.

Will CO_2 be fluid or solid at pressures (24–135 GPa) and temperatures (~1600–4200 K) of the Earth's lower mantle? The melting curve has been measured to 12 GPa (Giordano et al., 2006), i.e. at pressures where all solid phases are molecular. Its extrapolation (using Simon-Glatzel and Kechin equations) produces melting temperatures of only 1063 K at 24 GPa, 1408 K at 50 GPa and 2064 K at 135 GPa (i.e. below the geotherm) — a naïve interpretation of these numbers would lead one to conclude that CO_2 must be fluid. However, the extrapolation of the melting curve ignores the stability of dense non-molecular β-cristobalite polymorph, which may significantly increase the melting temperature[1] and make CO_2 solid at conditions of the Earth's mantle. In the absence of direct experimental or theoretical determinations of the melting curve at megabar pressures this question remains open.

3.3. High-pressure structures of $MgCO_3$

Experiments reported that magnesite is stable at least up to ~80 GPa (Fiquet et al., 2002) and transforms to a new phase above 100 GPa (Isshiki et al., 2004). However, the diffraction data up to now did not allow structure solution. Systematic search through databases of known crystal structures, combined with energy minimization, indicated that a pyroxene structure (space group $C2/c$) becomes energetically more favourable than magnesite above ~100 GPa (Skorodumova et al., 2005). This did not exclude the possibility of even better structures, and it soon turned out (Oganov et al., 2006) that the $C222_1$ structure (stable for $CaCO_3$) is more stable in a wide pressure range, but again still more stable structures could not be ruled out and several are actually found in this work — see below.

Isshiki et al. (Isshiki et al., (2004) have indexed their diffraction patterns in terms of an orthorhombic unit cell with 30 atoms. Our simulations using their lattice parameters demonstrate that their cell is unlikely: the resulting structures are energetically unfavourable and correspond to much higher pressures. Indexing of diffraction patterns with a small number of reflections is non-unique; besides, coexistence of several phases is possible in the sample.

To find stable post-magnesite structure(s), we performed fully unconstrained variable-cell USPEX simulations at 110 GPa and 150 GPa, using no experimental information such as lattice parameters or diffraction data. From the results we selected several best structures and explored their stability as a function of pressure.

Remarkably, we found many new low-enthalpy structures, which are more favourable than all previously known structures. The large number of energetically competitive structures for $MgCO_3$ under pressure (Fig. 4) suggests a very complex energy landscape, which can be problematic for evolutionary simulations, and therefore we cannot completely rule out the possibility of existence of slightly more favourable structures. Therefore a comparison with experiment is particularly important; here we perform it for the data of Isshiki et al. (2004) and for data collected in this work. Theoretically predicted low-enthalpy structures of $MgCO_3$ are shown in Fig. 5 and Table 1.

We find that between 82.4 GPa and 138.1 GPa the most stable structure has space group $C2/m$ and 30 atoms in the primitive cell; hereinafter we call it phase II. The most remarkable feature of the structure of phase II is the presence of three-membered rings $\{C_3O_9\}^{6-}$ made of carbonate tetrahedra (Fig. 5a). Mg atoms are in eight- and ten-fold coordinations. Above 138.1 GPa another structure is more stable, with space group $P2_1$ and also 30 atoms in the unit cell; we denote it phase III. Its structure has many similarities with phase II — three-membered $\{C_3O_9\}^{6-}$ rings (Fig. S3 in Supporting Online Material) and

[1] Because when a denser solid is formed, the slope of the melting curve $\frac{dT_m}{dP}=\frac{\Delta V_m}{\Delta S_m}$ increases.

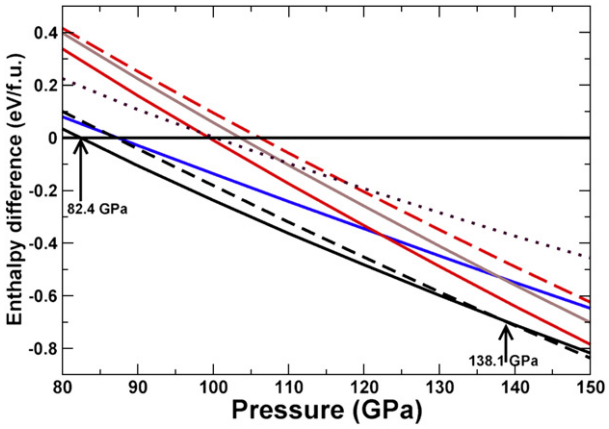

Fig. 4. Enthalpies of competitive $MgCO_3$ structures. Phase transition pressures are shown by the arrows. *Black solid line*: phase II, *black dashed*: phase III, *blue*: $P2_1$-10, *red solid*: $Pna2_1$-20, *red dashed*: $C222_1$, *black dotted: C2/c* pyroxene structure (Skorodumova et al., 2005), *gray solid line*: "edge-sharing" structure. Enthalpies are shown per formula unit and relative to magnesite.

Mg atoms in eight- and ten-fold coordinations (Fig. 5b). Although we did not perform any evolutionary simulations above 150 GPa (higher pressures are not relevant for the Earth's mantle, where the maximum pressure is 136 GPa), from the energetics of low-enthalpy structures found at 110 GPa and 150 GPa it appears that above ~160 GPa a $Pna2_1$ structure with 20 atoms/cell ($Pna2_1$-20), containing chains of corner-sharing carbonate tetrahedra, will be stable (Fig. 4).

Among low-enthalpy metastable structures, several deserve particular notice and are shown in Fig. 5. While most structures contain carbonate tetrahedra, one (with space group $P2_1$ and 10 atoms in the unit cell) contains triangular $(CO_3)^{2-}$ ions — but unlike in most low-pressure carbonates, these flat triangular ions are not coplanar. This structure type was previously found for a metastable form of $CaCO_3$ (Oganov et al., 2006). Another interesting structure, with the space group $Pna2_1$, contains chains of carbonate tetrahedra, and becomes the most stable structure above ~160 GPa (Fig. 4). The pyroxene structure proposed in (Skorodumova et al., 2005) is never thermodynamically stable. In the $P2_1$-10 and $Pna2_1$-20 structures, Mg atoms are in the ninefold coordination. One structure is especially remarkable — here, chains of corner-sharing CO_4-tetrahedra and pairs of edge-sharing tetrahedra coexist within the same structure. In Figs. 4 and 5 we denote this structure as "edge-sharing". For such small and highly charged cations as C^{4+}, sharing of polyhedral edges is forbidden by 3rd and 4th Pauling's rules — and yet, this structure has a remarkably low enthalpy (Fig. 4). Sharing of the tetrahedral edges leads to very short C–C distances: e.g., C–C=2.03 Å at 100 GPa.

To test our predictions, we have performed high-pressure experiments on $MgCO_3$. Experimental X-ray diffraction patterns are compared with theoretical ones in Fig. 6. The two experimental patterns obtained at 125 GPa and 119 GPa (this work and (Isshiki et al., 2004), respectively) have some similarities, but are clearly not identical. At these pressures, $MgCO_3$ has many energetically similar structures (Fig. 4), the relative stability of which may be easily changed by non-hydrostaticity and temperature. All diffraction peaks found in our experiments, except a few high-angle reflections, can be explained by a mixture of phase II and magnesite. This means that we now have a reasonable structural model for the post-magnesite phase, consistent with our experimental data — but more experimental work is clearly needed.

Increasing pressure, we indeed found a further phase transition, just as predicted by our simulations and occurring at a similar pressure (138 GPa in theory versus some pressure between 125–143 GPa in experiment). Many peaks in the experimental pattern can be explained by a mixture of phases II and III, but overall we do not observe very good agreement with experiment. This could indicate the presence of a metastable phase in the experiment or a ground state different from phase III. Metastability is likely to be a serious problem in experimental work on $MgCO_3$, and more experiments are needed. The experimental diffraction pattern contains lower-angle reflections (compared to Fig. 6a), which hints that the true crystal structure might have a larger unit cell (e.g., with 60 atoms in the unit cell). Treating such large cells within our evolutionary algorithm USPEX at the *ab initio* level is currently too expensive, but may become possible in the future. Usually, large-cell structures bring only slight (if any at all)

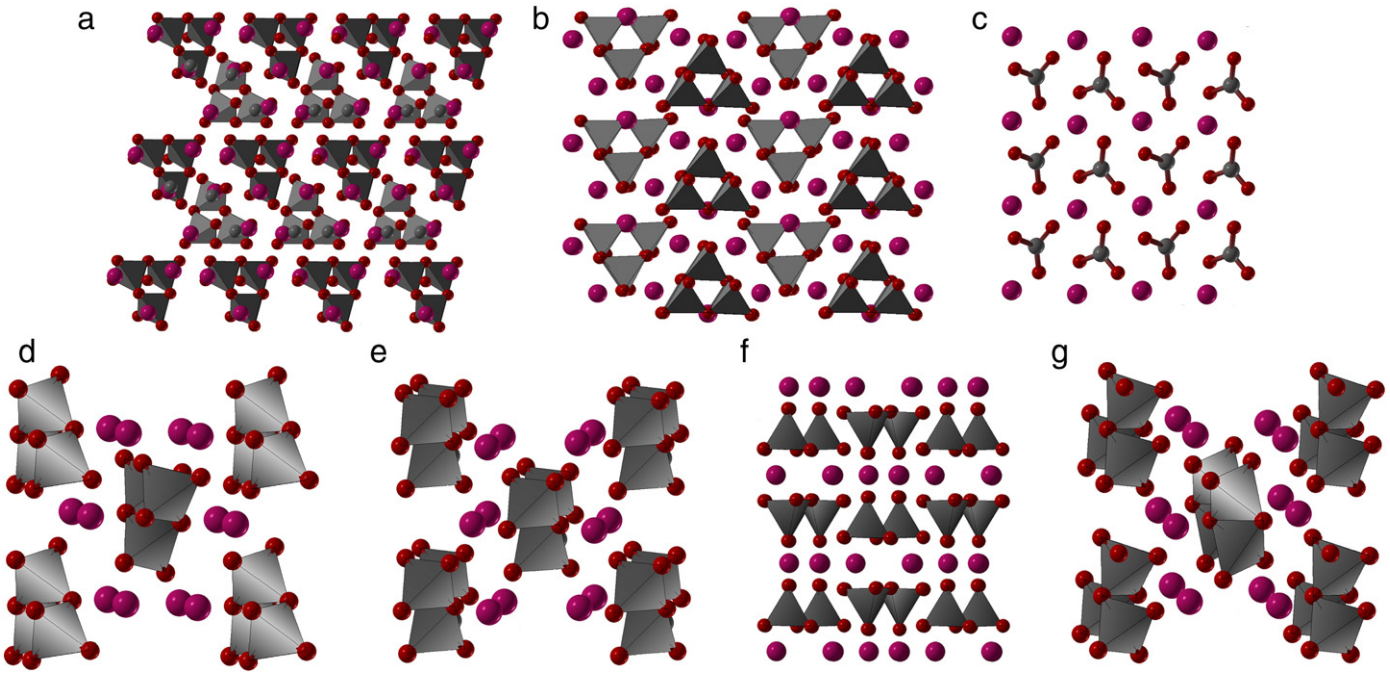

Fig. 5. Structures of low-energy phases of $MgCO_3$: a) phase II, b) phase III, c) $P2_1$-10 structure, d) $Pna2_1$-20 structure, e) $C222_1$ structure (the same structure type is shown in Fig. 1b), f) *C2/c* pyroxene structure (Skorodumova et al., 2005), g) "edge-sharing" structure.

Table 1
Crystal structures of $MgCO_3$ polymorphs at 120 GPa

Phase II. Space group $C2/m$, a=8.0945, b=6.4881, c=6.8795 Å, β=103.98			
	x	y	z
Mg1	0.00000	0.75372	0.00000
Mg2	0.32302	0.50000	−0.30268
Mg3	−0.06482	0.50000	−0.34569
C1	0.37049	0.32106	0.32672
C2	0.23155	0.50000	0.03550
O1	0.09256	0.50000	−0.10389
O2	0.34903	0.16655	0.42869
O3	0.50806	0.30973	0.26729
O4	0.36582	0.50000	−0.02754
O5	0.35178	0.50000	0.42732
O6	0.22500	0.33201	0.15891
Phase III. Space group $P2_1$, a=4.5338, b=7.7918, c=5.0864 Å, β=104.54°			
Mg1	−0.28603	−0.03307	0.73892
Mg2	0.26949	−0.20795	0.06204
Mg3	0.34823	0.12119	0.28515
C1	0.23144	0.44233	0.76917
C2	−0.13533	0.30299	0.44134
C3	0.18515	0.14122	0.78410
O1	0.15075	0.02103	0.94940
O2	0.43972	0.41714	0.63967
O3	0.05484	0.27607	0.29875
O4	−0.06009	0.45031	0.60657
O5	−0.40270	0.31481	0.28737
O6	−0.12259	0.16963	0.62513
O7	0.21551	0.29660	0.93081
O8	0.30108	0.57010	0.92898
O9	0.39421	0.13173	0.66211
Structure $P2_1$-10. Space group $P2_1$, a=2.6054, b=5.8921, c=3.9971 Å, β=106.26°			
Mg	0.7802	0.0795	0.5221
C	0.6544	0.3934	−0.0417
O1	0.6676	0.3724	0.2704
O2	0.3811	0.2668	−0.2725
O3	0.8870	0.5581	−0.1360
Bond lengths: Mg-O1=1.892, 1.977, 2.020 Å; Mg-O2=1.858, 1.903, 2.081 Å; Mg-O3=1.975, 1.979, 2.366 Å. C-O1=1.245 Å; C-O2=1.244 Å; C-O3=1.257 Å.			
Structure $Pna2_1$-20. Space group $Pna2_1$, a=7.1952, b=5.5687, c=2.8069 Å			
Mg	0.1868	0.4841	0.0517
C	0.0145	0.1642	0.7970
O1	−0.0784	0.3270	0.0267
O2	0.1528	0.2580	0.5699
O3	0.1067	−0.0210	0.0459
Bond lengths: Mg-O1=1.869, 1.972, 2.100, 2.421 Å; Mg-O2=1.864, 1.913, 1.939 Å; Mg-O3=2.033, 2.055 Å. C-O1=1.298 Å; C-O2=1.292 Å; C-O3=1.376, 1.411 Å.			

energetic improvements, therefore even if the ground state above 138 GPa is different from our phase III, we expect at least its energetics to be very similar. Furthermore, Fig. 4 shows that all candidate structures of $MgCO_3$ have very similar enthalpies and we expect that even if the true ground state structures differed from our predictions, the energetics of the $MgCO_3$ phases and reactions (R1a,b–R4) explored here would still be robust.

3.4. Crystal chemistry of tetrahedral carbonates

From the structures collected in Table 2 and Fig. 5, it is quite clear that structural chemistry of $MgCO_3$ and other carbonates at megabar pressures is based on CO_4-tetrahedra polymerised in chains or rings $(\{CO_3\}^{2-})_n$. This invites an analogy with silicates (chain and ring metasilicates), but the analogy is limited. In silicates, the intertetrahedral angle Si–O–Si is extremely flexible (Belov, 1961; Lasaga and Gibbs, 1987), which is one of the reasons for the enormous diversity of polysilicate structures and their high compressibility and easy glass formation. Fig. 7 shows the variation of the energy as a function of the Si–O–Si angle in the model $H_6Si_2O_7$ molecule — method borrowed from Lasaga and Gibbs (1987). What is striking is that the minimum at ∠(Si–O–Si)=135° is extremely shallow, i.e. there is little energy variation in a wide range of angles. For $H_6C_2O_7$ (Fig. 7) calculations show a different picture — a deep minimum at ∠(C–O–C)=124° with large energy variations accompanying small changes of the angle. This

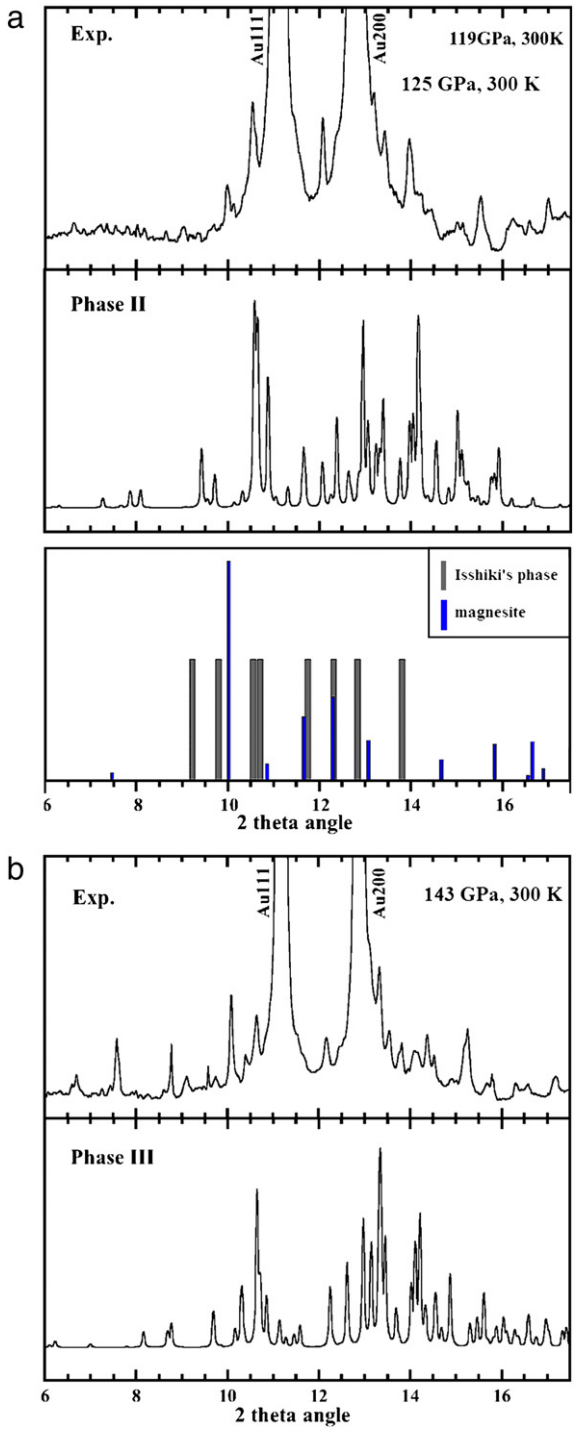

Fig. 6. X-ray powder diffraction patterns of post-magnesite phases of $MgCO_3$. a) experimental at 125 GPa and 300 K and theoretical at 120 GPa (X-ray wavelength λ=0.41103 Å), b) experimental at 143 GPa and 300 K and theoretical at 140 GPa (λ=0.41046 Å). Label "Au" in experimental data denotes diffraction peaks from gold. Lower panel in (a) shows diffraction peaks of magnesite (using the structure optimised at 120 GPa using the GGA) and Isshiki's phase ((Isshiki et al., 2004), at 119 GPa and 300 K, with reflections collected up to 2θ–14°).

Table 2
Summary of the high-pressure phases of $MgCO_3$, $CaCO_3$ and $SrCO_3$

		Pressure increases →						
		$(CO3)^{2-}$ triangles			$(C_3O_9)^{6-}$ rings of tetrahedra		Chains of CO_4-tetrahedra	
		Calcite CN(M)=6	Aragonite CN(M)=9	Post-aragonite CN(M)=12	Phase II CN(M)= 8 and 10	Phase III CN(M) = 8 and 10	*Pna*2_1-20 CN(M)=9	*C*222_1 CN(M)=10
Cation radius increases ↓	$MgCO_3$	0–82 GPa	–	–	82–138 GPa	138–160 GPa	>160 GPa	?
	$CaCO_3$	0–2 GPa	2–42 GPa	42–137 GPa	–	–	–	>137 GPa
	$SrCO_3$	–	0–10 GPa	>10 GPa	–	–	–	?
	$BaCO_3$	–	0–8 GPa	>8 GPa	–	–	–	–

CN(M) denotes the cation's coordination number.

suggests that polycarbonate ions are much less flexible, and one expects a much more limited structural variability for tetrahedral carbonates, lower compressibility and lower propensity to amorphisation than for their silicate counterparts.[2] The optimal angle ∠(*C*–O–*C*)= 124° is naturally accommodated by chain polyanions and trigonal $(C_3O_9)^{6-}$ and hexagonal $(C_3O_9)^{12-}$ ring polyanions. The chain polyanions are present in the *C*222_1 phase of $CaCO_3$, the trigonal rings exist in both of the post-magnesite phases predicted here, and hexagonal rings may be present in other carbonates (perhaps in $MnCO_3$, the high-pressure phase of which is likely to have a complicated structure with a large unit cell (Ono, 2007)).

In the tetrahedral carbonate structures explored here (CO_2-V, *C*222_1 $CaCO_3$, and $MgCO_3$ phases II and III and *C*222_1 and *Pna*2_1 structures) the values of the ∠(*C*–O–*C*) angles are all in the range 115°–125° at atmospheric pressure, but they decrease to 112°–115° at 100 GPa. In contrast to the relatively constant C–O–C angles, the C–O distances within the tetrahedra show surprisingly large distortions, bridging C–O distances being always longer (by ~0.06–0.10 Å — see Fig. S3 in Supporting Online Material) than the non-bridging ones. This distortion is also found for the $H_6C_2O_7$ molecule, and for solid phases remains the same up to the highest pressure studied here (200 GPa). There is no such distortion in the CO_2-V structure, where all distances are bridging and symmetrically equivalent. The different flexibility of the C–O–C and Si–O–Si angles suggests that the analogy between silicates and tetrahedral carbonates is very limited — indeed, high-pressure structures of CO_2, $CaCO_3$ and $MgCO_3$ are very different from the stable structures of SiO_2, $CaSiO_3$ and $MgSiO_3$.

Because of the limited flexibility of the C–O–C angles, tetrahedral carbonates are stiffer than their silicate counterparts — e.g., the zero-pressure bulk modulus of CO_2-V is 115 GPa (Table S1 in Supporting Online Material), much higher than that of SiO_2 quartz (37.5 GPa) (Calderon et al., 2007). The extremely high bulk modulus of 365 GPa, proposed for CO_2-V in (Yoo et al., 1999), does not agree with our findings and with previous works (Holm et al., 2000; Dong et al., 2000).

With the results obtained here and in (Oganov et al., 2006; Isshiki et al., 2004; Ono et al., 2005a,b, 2007, submitted for publication; Ono, 2007), we can present an updated structural sequences for carbonates under pressure (Table 2). Clearly, there are large differences between $MgCO_3$ and $CaCO_3$ under pressure, and these can be traced to the differences in the ionic radii: while Ca^{2+} has an ionic radius similar to that of O^{2-} and can adopt high coordination numbers (up to 12 in post-aragonite), Mg^{2+} is substantially smaller and has lower coordination numbers (only up to 10 in this pressure range). Mn^{2+}, which possesses an ionic radius intermediate between the radii of Mg^{2+} and Ca^{2+}, seems to have more similarity to $MgCO_3$, but the structures of its high-pressure phases are unknown (Ono, 2007). For $FeCO_3$ one can expect similarly complex behaviour. Spin transitions of Mn^{2+} and Fe^{2+} under pressure can further complicate the high-pressure chemistry of $MnCO_3$ and $FeCO_3$. The trends emerging from Table 2 can be summarized as follows: cation coordination numbers and the degree of polymerization of the anions increase with cation's radius — just as one would expect from Pauling's first rule and from Belov's principle (formulated originally for silicates — Belov, 1961).

3.5. Carbon storage in the lower mantle and the possibility of producing free CO2

It has been argued (Isshiki et al., 2004 and references therein) that $MgCO_3$ should be the main host of oxidised carbon in the Earth's mantle. We would like to check this by looking at the energetics of the reactions (R3, R4). Furthermore, we explore the possibility of producing free CO_2 in the mantle by modelling reactions (R1a,b–R2a,b).

In calculations of these reactions we used the stable structures at each pressure (see Oganov et al., 2005b; Oganov and Ono, 2004; Jung and Oganov, 2005). Having included the stable forms of carbon (diamond) and oxygen (Ma et al., 2007) in the calculations, we made sure that CO_2 is stable to decomposition into these elements (the enthalpy of its decomposition increases from 3.3 eV to 3.8 eV between 50 GPa and 200 GPa)[3,4]. The calculated enthalpies of reactions (R1a, b–R4) (Fig. 8) lead us to the following conclusions:

(i) Neither $MgCO_3$ nor $CaCO_3$ are likely to decompose into the oxides (reactions R1a and R1b, Fig. 8a) in the explored pressure range.
(ii) Through most of the Earth's mantle, $MgCO_3$ should be the dominant host of oxidised carbon. Only above 136 GPa would $CaCO_3$ appear (reaction R3). Given the smallness of the enthalpy of reaction (R3), temperature and chemical potentials may conceivably shift the stability field of $CaCO_3$ to significantly lower or higher pressures.
(iii) In SiO_2-rich subducted basalts, both $MgCO_3$ and $CaCO_3$ (reactions R2a and R2b, respectively) should react with SiO_2 at pressures above 137 GPa, producing free CO_2. If CO_2 is fluid at mantle temperatures, the reaction may take place at lower pressures. There is an experimental report (Takafuji et al., 2006) of such a reaction at 28–62 GPa and 1490–2000 K.

Point (iii) is particularly interesting: it implies that subducted slabs can produce large amounts of CO_2 right at the core-mantle boundary (where the pressure is 136 GPa). If CO_2 is indeed in the fluid form, it can play an important role, enhancing partial melting and chemical equilibration at the core-mantle boundary. Such fluids as CO_2 and H_2O, contributing to the rheological weakening of mantle rocks, may be an important prerequisite of plate tectonics and their presence/absence in planetary interiors could be the key to explaining differences in the

[2] Note, however, the recent discovery of an amorphous phase of CO_2 with tetrahedral coordination of carbon atoms (Santoro et al., 2006).

[3] Using extrapolation of thermodynamic functions of magnesite, periclase (MgO) and fluid CO_2, Dorogokupets (2007) arrived at the same conclusion — i.e. that $MgCO_3$ remains stable to decomposition at conditions of the lower mantle.

[4] In an open thermodynamic system with strongly reducing conditions, it may be possible to decompose CO_2 — for instance, in reactions $CO_2+2Fe=C+2FeO$ and $CO_2+5Fe=Fe_3C+2FeO$, which our GGA calculations indicate as favourable at high pressure.

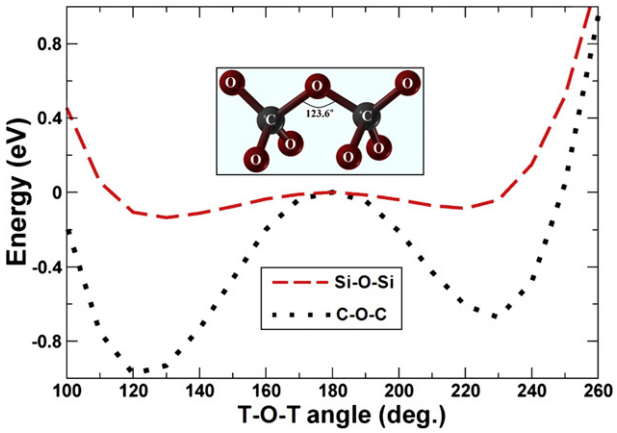

Fig. 7. Energy variation as a function of the T–O–T angle. *Red dashed line*: T=Si, *black dotted line:* T=C. Calculations were performed on $H_6T_2O_7$ molecules (as in Lasaga & Gibbs, 1987); at each angle all T–O distances and O–T–O valence angles were optimised. The inset shows molecular geometry used in calculations. Optimum angle C–O–C=124°, Si–O–Si=135°. These calculations were performed with SIESTA code (Soler et al., 2002) using the GGA functional (Perdew et al., 1996), norm-conserving pseudopotentials and a double-ζ basis set with a single polarisation function for each atom.

dynamics of the Earth and other terrestrial planets — Mercury, Venus and Mars (which are smaller and are expected to have lower maximal pressures in their mantles). The Earth corresponds to a nearly critical size, below which deep internal production of CO_2 is unlikely.

In experiments (Takafuji et al., 2006) production of CO_2 through reaction (R2a) was observed at much lower pressures (28–62 GPa) than predicted here. Unlike the experiment, our calculations are done at T=0 K, but given the large values of the reaction enthalpy (Fig. 8b), it is unlikely that temperature can shift reaction pressure so as to agree with experiment (Takafuji et al., 2006). In some of the experimental runs (Takafuji et al., 2006) diamond and oxygen were found instead of CO_2, a mixture which according to our calculations is extremely unfavourable in comparison with CO_2 (see above). We believe that this is a sign of non-equilibrium conditions in the experiment. A similar situation occurred with $MnCO_3$, for which earlier experiments (Liu et al., 2001) reported pressure-induced decomposition producing diamond, but later experiments (Ono, 2007) found no decomposition.

4. Summary

We have presented theoretical and experimental evidence that above 82 GPa $MgCO_3$ adopts a new complex structure (phase II) containing $(C_3O_9)^{6-}$ rings of carbonate tetrahedra. This structure, predicted using our evolutionary algorithm USPEX (Oganov et al., 2006; Oganov and Glass, 2006; Glass et al., 2006), was also confirmed by high-pressure experiments performed here. We also predicted that above 138 GPa another phase will become stable; our experiments confirmed this prediction, but the structure of the new phase is not fully established.

For CO_2, our evolutionary simulations confirm stability of the tetragonal (space group $I\bar{4}2d$) β-cristobalite structure from 19 GPa up to at least 150 GPa, in agreement with (Holm et al., 2000; Dong et al., 2000). At all these pressures, CO_2 is stable to decomposition into elemental carbon and oxygen.

We showed that in the high-pressure tetrahedral carbonates, the intertetrahedral C–O–C angles are much more rigid than the Si–O–Si angles in silicates. This explains the structural differences between high-pressure carbonates and low-pressure silicates, and suggests that tetrahedral carbonates should have much less structural variability and lower compressibilities than silicates.

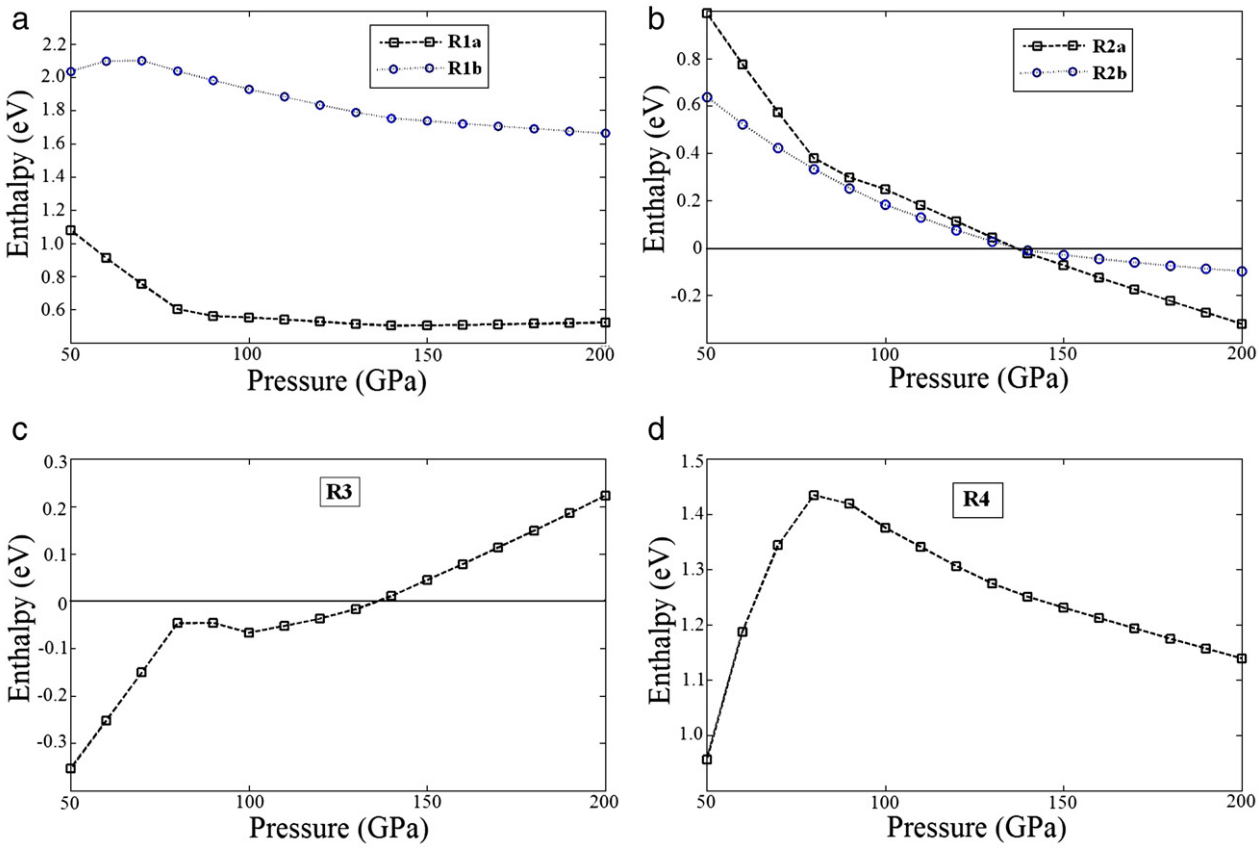

Fig. 8. Enthalpies of reactions (R1a,b–R4) as a function of pressure. Lines are guides to the eye only.

We have shown that $MgCO_3$ is preferable to $CaCO_3$ as the main host of oxidised carbon in the Earth's lower mantle. Only in the lowermost part of the mantle can $CaCO_3$ become preferable, as the enthalpy of reaction (R3) changes sign from negative to positive at ~135 GPa:

$$CaCO_3 + MgSiO_3 = CaSiO_3 + MgCO_3 \quad (R3)$$

According to our calculations, neither $MgCO_3$ nor $CaCO_3$ should decompose into the oxides at lower mantle *P–T* conditions. However, there are two reactions that can produce free CO_2 in the lower mantle:

$$MgCO_3 + SiO_2 = MgSiO_3 + CO_2 \quad (R2a)$$

$$CaCO_3 + SiO_2 = CaSiO_3 = CO_2 \quad (R2b)$$

Both reactions are thermodynamically favourable above ~135 GPa and therefore are only viable in the lowermost mantle. Both occur in excess of silica (which is not expected in normal mantle) and therefore free CO_2 may be produced only in small silica-rich basaltic parts of the subducted slabs. These parts are also rich in carbonates, and may correspond to narrow zones of intense CO_2 production at the bottom of the Earth's mantle. It is unknown whether at conditions of the lowermost mantle CO_2 is fluid (in which case it may induce partial melting and significantly affect rheological behaviour of mantle rocks) or solid (i.e. a new mineral phase in the mantle).

Acknowledgments

Calculations were performed at CSCS (Manno), at the Joint Supercomputer Centre of Russian Academy of Sciences, at ETH Zurich and on the Skif Cyberia supercomputer of Tomsk State University (Russia). ARO gratefully acknowledges financial support from the Swiss National Science Foundation (grant 200021-111847/1) and ETH Zurich Research Equipment Programme. The synchrotron radiation experiments were performed at the PF, KEK (Proposal No. 2005G122) and at the Spring-8 (Proposal No. 2006A1412). AG acknowledges the support of the Spanish Ministry of Education (grants MAT2005-05216 and FIS2006-12117-C04-01) and the hospitality of ETH Zurich. We thank R. Martonak for providing metadynamics routines, D. Vicente (Barcelona Supercomputer Centre), T. Racic, G. Sigut, A. Bongulielmi, N. Stringfellow and M. Valle for technical support. ARO thanks M. Hirschmann, T.S. Duffy, A. Kubo and F. Liebau for stimulating discussions.

Appendix A. Supplementary data

Supplementary data associated with this article can be found, in the online version, at doi:10.1016/j.epsl.2008.06.005.

References

Arapan, S., Souza de Almeida, J., Ahuja, R., 2007. Formation of sp^3 hybridized bonds and stability of $CaCO_3$ at very high pressure. Phys. Rev. Lett. 98 art. 268501.
Belov, N.V., 1961. Crystal Chemistry of Silicates with Large Cations. Russian Academy of Sciences Press, Moscow [in Russian].
Blöchl, P.E., 1994. Projector augmented-wave method. Phys. Rev. B50, 17953–17979.
Bonev, S.A., Gygi, F., Ogitsu, T., Galli, G., 2003. High-pressure molecular phases of solid carbon dioxide. Phys. Rev. Lett. 91, 065501.
Brenker, F.E., Vollmer, C., Vincze, L., Vekemans, B., Szymanski, A., Janssens, K., Szaloki, I., Nasdala, L., Joswig, W., Kaminsky, F., 2007. Carbonates from the lower part of transition zone or even the lower mantle. Earth Planet. Sci. Lett. 260, 1–9.
Calderon, F., Gauthier, M., Decremps, F., Hamel, G., Syfosse, G., Polian, A., 2007. Complete determination of the elastic moduli of alpha-quartz under hydrostatic pressure up to 1 GPa: an ultrasonic study. J. Phys.: Cond. Matter 19 art. 436228.
Day, G.M., Motherwell, W.D.S., Ammon, H.L., Boerrigter, S.X.M., Della Valle, R.G., Venuti, E., Dzyabchenko, A., Dunitz, J.D., Schweizer, B., van Eijck, B.P., Erk, P., Facelli, J.C., Bazterra, V.E., Ferraro, M.B., Hofmann, D.W.M., Leusen, F.J.J., Liang, C., Pantelides, C.C., Karamertzanis, P.G., Price, S.L., Lewis, T.C., Nowell, H., Torrisi, A., Scheraga, H.A., Arnautova, Y.A., Schmidt, M.U., Verwer, P., 2005. A third blind test of crystal structure prediction. Acta Cryst. B61, 511–527.
Dong, J.J., Tomfohr, J.K., Sankey, O.F., Leinenweber, K., Somayazulu, M., McMillan, P.F., 2000. Investigation of hardness in tetrahedrally bonded nonmolecular CO2 solids by density-functional theory. Phys. Rev. B62, 14685–14689.
Dorogokupets, P.I., 2007. Equation of state of magnesite for the conditions of the Earth's lower mantle. Geochem. Int. 45, 561–568.
Dorogokupets, P.I., Oganov, A.R., 2007. Ruby, metals, and MgO as alternative pressure scales: a semiempirical description of shock-wave, ultrasonic, X-ray, and thermochemical data at high temperatures and pressures. Phys. Rev. B75 art. 024115.
Fiquet, G., Guyot, F., Kunz, M., Matas, J., Andrault, D., Hanfland, M., 2002. Structural refinements of magnesite at very high pressure. Am. Mineral. 87, 1261–1265.
Frost, D.J., Liebske, C., Langenhorst, F., McCammon, C.A., Tronnes, R.G., Rubie, D.C., 2004. Experimental evidence for the existence of iron-rich metal in the Earth's lower mantle. Nature 428, 409–412.
Giordano, V.M., Datchi, F., Dewaele, A., 2006. Melting curve and fluid equation of state of carbon dioxide at high pressure and high temperature. J. Chem. Phys. 125 art. 054504.
Glass, C.W., Oganov, A.R., Hansen, N., 2006. USPEX — evolutionary crystal structure prediction. Comput. Phys. Commun. 175, 713–720.
Holm, B., Ahuja, R., Belonoshko, A., Johansson, B., 2000. Theoretical investigation of high pressure phases of carbon dioxide. Phys. Rev. Lett. 85, 1258–1261.
Isshiki, M., Irifune, T., Hirose, K., Ono, S., Ohishi, Y., Watanuki, T., Nishibori, E., Takadda, M., Sakata, M., 2004. Stability of magnesite and its high-pressure form in the lowermost mantle. Nature 427, 60–63.
Jung, D.Y., Oganov, A.R., 2005. *Ab initio* study of the high-pressure behaviour of $CaSiO_3$ perovskite. Phys. Chem. Minerals 32, 146–153.
Kresse, G., Furthmüller, J., 1996. Efficient iterative schemes for *ab initio* total-energy calculations using a plane wave basis set. Phys. Rev. B54, 11169–11186.
Kresse, G., Joubert, D., 1999. From ultrasoft pseudopotentials to the projector augmented-wave method. Phys. Rev. B59, 1758–1775.
Lasaga, A.C., Gibbs, G.V., 1987. Applications of quantum-mechanical potential surfaces to mineral physics calculations. Phys. Chem. Minerals 14, 107–117.
Liu, L.G., Lin, C.C., Yang, Y.J., 2001. Formation of diamond by decarbonation of $MnCO_3$. Solid St. Comm. 118, 195–198.
Luth, R.W., 1999. Carbon and carbonates in the mantle. In: Fei, Y., Bertka, C.M., Mysen, B.O. (Eds.), Mantle Petrology: Field Observations and High Pressure Experimentation: A Tribute to Francis R. (Joe) Boyd. Geochemical Soc., vol. 6. Special Publication.
Ma, Y., Oganov, A.R., Glass, C.W., 2007. Structure of the metallic ζ-phase of oxygen and isosymmetric nature of the ε-ζ phase transition: *ab initio* simulations. Phys. Rev. B76 art. 064101.
Maddox, J., 1988. Crystals from first principles. Nature 335, 201.
Martinez, I., Zhang, J., Reeder, R.J., 1996. In situ X-ray diffraction of aragonite and dolomite at high pressure and high temperature: evidence for dolomite breakdown to aragonite and magnesite. Am. Mineral. 81, 611–624.
Martoňák, R., Laio, A., Parrinello, M., 2003. Predicting crystal structures: the Parrinello–Rahman method revisited. Phys. Rev. Lett. 90 art. 075503.
Martoňák, R., Laio, A., Bernasconi, M., Ceriani, C., Raiteri, P., Zipoli, F., Parrinello, M., 2005. Simulation of structural phase transitions by metadynamics. Z. Krist. 220, 489–498.
Martoňák, R., Donadio, D., Oganov, A.R., Parrinello, M., 2006. Crystal structure transformations in SiO_2 from classical and *ab initio* metadynamics. Nature Materials 5, 623–626.
Oganov, A.R., Ono, S., 2004. Theoretical and experimental evidence for a post-perovskite phase of MgSiO3 in Earth's D″ layer. Nature 430, 445–448.
Oganov, A.R., Glass, C.W., 2006. Crystal structure prediction using *ab initio* evolutionary algorithms: principles and applications. J. Chem. Phys. 124 art. 244704.
Oganov, A.R., Glass, C.W., Ono, S., 2006. High-pressure phases of CaCO3: crystal structure prediction and experiment. Earth Planet. Sci. Lett. 241, 95–103.
Oganov, A.R., Martoňák, R., Laio, A., Raiteri, P., Parrinello, M., 2005a. Anisotropy of Earth's D″ layer and stacking faults in the $MgSiO_3$ post-perovskite phase. Nature 438, 1142–1144.
Oganov, A.R., Gillan, M.J., Price, G.D., 2005b. Structural stability of silica at high pressures and temperatures. Phys. Rev. B71 art. 064104.
Oganov, A.R., Gatti, C., Glass, C.W., Ma, Y.Z., Ma, Y.M., Chen, J., submitted for publication. Ionic high-pressure form of elemental boron.
Ono, S., 2007. High-pressure phase transformation in $MnCO_3$: a synchrotron XRD study. Min. Mag. 71, 105–111.
Ono, S., Shirasaka, M., Kikegawa, T., Ohishi, Y., 2005a. A new high-pressure phase of strontium carbonate. Phys. Chem. Minerals 32, 8–12.
Ono, S., Kikegawa, T., Ohishi, Y., Tsuchiya, J., 2005b. Post-aragonite phase transformation in $CaCO_3$ at 40 GPa,. Am. Mineral. 90, 667–671.
Ono, S., Kikegawa, T., Ohishi, Y., 2007. High-pressure phase transition of $CaCO_3$. Am. Mineral. 92, 1246–1249.
Ono, S., Brodholt, J.P., Price, G.D., submitted for publication. Phase transitions of $BaCO_3$ at high pressures.
Ono, S., Oganov, A.R., Brodholt, J.P., Vocadlo, L., Wood, I.G., Glass, C.W., Côté, A.S., Price, G.D., in press. High-pressure phase transformations of FeS: novel phases at conditions of planetary cores. Earth Planet. Sci. Lett.
Perdew, J.P., Burke, K., Ernzerhof, M., 1996. Generalized gradient approximation made simple. Phys. Rev. Lett. 77, 3865–3868.
Santillán, J., Williams, Q., 2004. A high pressure X-ray diffraction study of aragonite and the post-aragonite phase transition in $CaCO_3$. Am. Mineral. 89, 1348–1352.
Santoro, M., Gorelli, F.A., Bini, R., Ruocco, G., Scandolo, S., Crichton, W.A., 2006. Amorphous silica-like carbon dioxide. Nature 441, 857–860.
Sato, K., Katsura, T., 2001. Experimental investigation on dolomite dissociation into aragonite-magnesite up to 8.5 GPa. Earth Planet. Sci. Lett. 184, 529–534.
Scott, H.P., Williams, Q., Knittle, E., 2001. Stability and equation of state of Fe_3C to 73 GPa: implications for carbon in the Earth's core. Geoph. Res. Lett. 28, 1875–1878.
Shcheka, S.S., Wiedenbeck, M., Frost, D.J., Keppler, H., 2006. Carbon solubility in mantle minerals. Earth Planet. Sci. Lett. 245, 730–742.

Shirasaka, M., Takahashi, E., Nishihara, Y., Matsukage, K., Kikegawa, T., 2002. In situ X-ray observation of the reaction dolomite = aragonite + magnesite at 900–1300 K. Am. Mineral. 87, 922–930.

Skorodumova, N.V., Belonoshko, A.B., Huang, L., Ahuja, R., Johansson, B., 2005. Stability of the $MgCO_3$ structures under lower mantle conditions. Am. Mineral. 90, 1008–1011.

Soler, J.M., Artacho, E., Gale, J.D., Garcia, A., Junquera, J., Ordejon, P., Sanchez-Portal, D., 2002. The SIESTA method for *ab initio* order-N materials simulation. J. Phys.: Condens. Matter 14, 2745–2779.

Suito, K., Namba, J., Horikawa, T., Taniguchi, Y., Sakurai, N., Kobayashi, M., Onodera, A., Shimomura, O., Kikegawa, T., 2001. Phase relations of $CaCO_3$ at high pressure and high temperature. Am. Mineral. 86, 997–1002.

Takafuji, N., Fujino, K., Nagai, T., Seto, Y., Hamane, D., 2006. Decarbonation reaction of magnesite in subducting slabs at the lower mantle. Phys. Chem. Minerals 33, 651–654.

Yoo, C.S., Cynn, H., Gygi, F., Galli, G., Iota, V., Nicol, M., Carlson, S., Hausermann, D., Mailhiot, C., 1999. Crystal structure of carbon dioxide at high pressure: “superhard” polymeric carbon dioxide. Phys. Rev. Lett. 83, 5527–5530.

Zhang, F., Oganov, A.R., 2006. Valence and spin states of iron impurities in mantle-forming silicates. Earth Planet. Sci. Lett. 249, 436–443.